ResearchGate

See discussions, stats, and author profiles for this publication at: https://www.researchgate.net/publication/263609122

The C-terminal transmembrane domain of human phospholipid scramblase 1 is essential for the protein flip-flop activity and Ca2+-binding

ARTICLE *in* JOURNAL OF MEMBRANE BIOLOGY · FEBRUARY 2014

Impact Factor: 2.46 · DOI: 10.1007/s00232-013-9619-7

CITATIONS
5

READS
46

9 AUTHORS, INCLUDING:

Lissete Sánchez-Magraner
University of Verona
13 PUBLICATIONS **241** CITATIONS
SEE PROFILE

F-Xabier Contreras
Universidad del País Vasco / Euskal Herriko…
20 PUBLICATIONS **554** CITATIONS
SEE PROFILE

Diego Guérin
Universidad del País Vasco / Euskal Herriko…
43 PUBLICATIONS **312** CITATIONS
SEE PROFILE

Hugo L Monaco
University of Verona
96 PUBLICATIONS **2,657** CITATIONS
SEE PROFILE

All in-text references underlined in blue are linked to publications on ResearchGate, letting you access and read them immediately.

Available from: Diego Guérin
Retrieved on: 13 January 2016

Biochimica et Biophysica Acta 1798 (2010) 1225–1233

Contents lists available at ScienceDirect

Biochimica et Biophysica Acta

journal homepage: www.elsevier.com/locate/bbamem

Interdomain Ca^{2+} effects in *Escherichia coli* α-haemolysin: Ca^{2+} binding to the C-terminal domain stabilizes both C- and N-terminal domains

Lissete Sánchez-Magraner, Aitziber L. Cortajarena, Marcos García-Pacios, José-Luis R. Arrondo, Jon Agirre, Diego M.A. Guérin, Félix M. Goñi, Helena Ostolaza *

Unidad de Biofísica (Centro Mixto CSIC-UPV/EHU), and the Departamento de Bioquímica, Universidad del País Vasco, Aptdo. 644, 48080 Bilbao, Spain

ARTICLE INFO

Article history:
Received 4 December 2009
Received in revised form 8 February 2010
Accepted 3 March 2010
Available online 16 March 2010

Keywords:
Membrane-targeted protein toxins
Calcium-binding domains
RTX toxin family
Protein stability
Urea denaturation
Amphipathic proteins

ABSTRACT

α-Haemolysin (HlyA) is a toxin secreted by pathogenic *Escherichia coli*, whose lytic activity requires submillimolar Ca^{2+} concentrations. Previous studies have shown that Ca^{2+} binds within the Asp and Gly rich C-terminal nonapeptide repeat domain (NRD) in HlyA. The presence of the NRD puts HlyA in the RTX (Repeats in Toxin) family of proteins. We tested the stability of the whole protein, the amphipathic helix domain and the NRD, in both the presence and absence of Ca^{2+} using native HlyA, a truncated form of HlyAΔN601 representing the C-terminal domain, and a novel mutant HlyA W914A whose intrinsic fluorescence indicates changes in the N-terminal domain. Fluorescence and infrared spectroscopy, tryptic digestion, and urea denaturation techniques concur in showing that calcium binding to the repeat domain of α-haemolysin stabilizes and compacts both the NRD and the N-terminal domains of HlyA. The stabilization of the N-terminus through Ca^{2+} binding to the C-terminus reveals long-range inter-domain structural effects. Considering that RTX proteins consist, in general, of a Ca^{2+}-binding NRD and separate function-specific domains, the long-range stabilizing effects of Ca^{2+} in HlyA may well be common to other members of this family.

© 2010 Elsevier B.V. All rights reserved.

1. Introduction

α-Haemolysin (HlyA) is a protein toxin (1024 amino acid residues) responsible for the pathogenic properties of some *Escherichia coli* strains that infect the urinary tract. HlyA is secreted to the aqueous medium in both soluble and vesicular forms [1], where it binds target membranes causing impairment of cell function, and even cell lysis. Importantly, HlyA is a member of a protein family characterized by a set of 11–17 glycine- and aspartate-rich nonapeptide tandem repeats, depending on how much deviation is allowed from the consensus sequence. Some, but not all, members of this family are bacterial toxins, hence the name RTX (repeats in toxin) which is often given to the family [2].

The nonapeptide repeat domain (NRD) makes up the bulk of the C-terminal region of HlyA (Scheme 1). It has been shown that Ca^{2+}, a cation essential for protein function, is bound by this domain [3]. Further, the NRDs of several proteins belonging to this family have been studied by X-ray crystallography and their structures determined to atomic resolution [4–6]. In the presence of Ca^{2+}, the NRD assembles into a β-roll structure, in which the first six residues of this sequence motif form a loop and the last three form a short β-strand. Each Ca^{2+} ion binds a pair of these loops. In general, the N-terminal domain of HlyA, which contains nine amphipathic helices [7,8], is considered to be the main anchor of the toxin to the target membranes. However, recent evidence [9] points to the NRD as the HlyA region that binds the membrane at an early stage.

Previous studies from this laboratory [7] have shown that Ca^{2+} binding to the C-terminal region of native HlyA made the protein more stable against denaturation. It has also been proposed [7,10] that Ca^{2+} binding did not induce significant changes in the secondary structure of HlyA, but rather that the tertiary structure is modified as a result of Ca^{2+} binding, and that the structural effects are transmitted to the N-terminal region. This would result in the hydrophobic regions being exposed to the surface of the protein giving rise to some kind of metastable conformation that facilitates either self-aggregation or membrane insertion [3,10,11].

In a previous paper [9], we described the cloning and purification of a truncated HlyA mutant, HlyAΔN601, consisting largely of the NRD. HlyAΔN601 was found to be a potent surface-active protein, which was unexpected given that this role in HlyA had been traditionally assigned to the N-terminal end, containing the amphipathic helices. The NRD bound Ca^{2+} with about the same affinity as the parent protein ($K_{0.5} \approx 10^{-4}$ M), and the Ca^{2+} made the protein

Abbreviations: TC buffer, 150 mM NaCl, 20 mM Tris, pH = 7; TH buffer, 150 mM NaCl, 10 mM $CaCl_2$, 20 mM Tris, pH = 7; TCU buffer, 6 M urea, 150 mM NaCl, 20 mM Tris, pH = 7

* Corresponding author. Unidad de Biofísica (Centro Mixto CSIC-UPV/EHU), and the Departamento de Bioquímica, Universidad del País Vasco, Aptdo. 644, 48080 Bilbao, Spain. Tel.: +34 94 6012625; fax: +34 94 601 33 60.
E-mail address: gbzoseth@ehu.es (H. Ostolaza).

0005-2736/$ – see front matter © 2010 Elsevier B.V. All rights reserved.
doi:10.1016/j.bbamem.2010.03.007

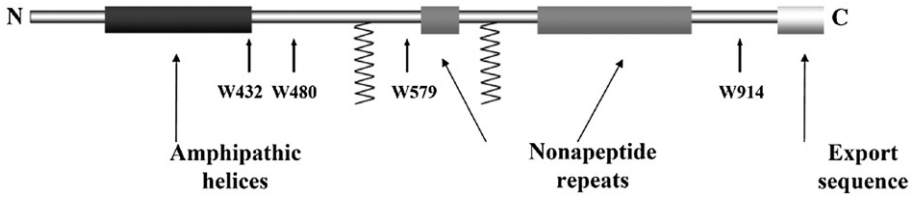

Scheme 1. (A) An outline of HlyA structure. Fatty acids bound to Lys-564 and Lys-690 are also indicated. (B) An outline of the truncated mutant of HlyA, protein HlyAΔN601 structure.

adopt a more periodic structure, with a higher β-sheet content [9]. The related NRD of *Bordetella pertussis* adenylate cyclase toxin has also been cloned and expressed [12] and it was found that Ca^{2+} binding had the effect of increasing the proportion of periodically structured elements in the protein.

Consequently, we decided to explore in detail the effects of Ca^{2+} ions on the stability of the N-terminal and C-terminal domains. To this end, a variety of assays were performed using, apart from native HlyA, the HlyAΔN601 mutant representing the C-terminal region, and a novel mutant HlyA W914A. The latter mutant lacks the only Trp residue in the C-terminal domain, and hence intrinsic fluorescence emission from HlyA W914A mainly indicates events involving the N-terminal moiety. Using a combination of enzymatic, spectroscopic and chromatographic methods we investigated the ways in which Ca^{2+}-binding makes the NRD more compact, more thermally stable, and less hydrophobic. Moreover, urea-induced unfolding of the native and mutant forms of HlyA would demonstrate that in the presence of Ca^{2+} the whole protein gains stability. We propose that, in the native protein, Ca^{2+}-induced changes in the NRD are transmitted to the amphipathic helix domain with the final outcome that this domain also becomes stabilized.

2. Material and methods

2.1. Site-directed mutagenesis of HlyA

The substitution of codon Trp 914 by Ala was introduced into the *hlyA* gene by sequential PCR steps. In the first step, fragments upstream and downstream of the point mutation were PCR-amplified, in two separate reactions, using the flanking primers and oligonucleotides containing the point mutation to be introduced. The two fragments, partially overlapping, encompassing the mutation were combined in an overlap extension reaction with the flanking primers. The full-length mutagenized fragment generated in this way was digested with *Nco*I and *Pac*I and cloned into pSU124 restricted with the same restriction enzymes. The resulting plasmid contained an inserted fragment identical to the original DNA except for the substitution W914A. Mutations were confirmed by DNA sequencing.

Flanking primers:

5′ GATATCTTCCATGGCGCGG 3′
5′ GATTTCATTAATTAATGGATTA 3′

Mutagenic primers: W914A

5′ CTTTTTCAAATGCGTTCCTGAA 3′
5′ TTCAGGAACGCATTTGAAAAAG 3′

2.2. Protein purification

Wild-type and mutant HlyAW914A were purified as described previously for the wild type by Ostolaza et al. [3]. The truncated mutant HlyAΔN601 was purified using an ionic exchange column of DEAE Sepharose, following the method of Sanchez-Magraner et al. [9].

2.3. ANS binding to HlyAΔN601

Binding of the fluorescent probe 1,8-ANS (*1-anilino*-naphthalene-*8*-sulfonate) was used to detect hydrophobic regions on the protein surface. Protein samples were diluted to 1 μM, in 150 mM NaCl, 20 mM Tris, pH = 7 buffer (TC buffer) in the absence (control) or presence of 10 mM calcium. Then small aliquots of an ANS solution were successively added. After each addition the mixture was incubated with continued stirring for 5 min (sufficient time to reach equilibrium). The fluorescence emission spectra were recorded with $\lambda_{ex} = 360$ nm and $\lambda_{em} = 430–600$ nm and the measurements were corrected using a blank without protein.

The calibration factor ($\Delta F_{max}/[ANS]$) that relates the changes in fluorescence intensity to the amount of ANS bound to the protein was determined by a reverse titration method. The protocol of this particular experiment makes impossible to perform a centrifugation step simultaneously for each protein concentration, as the increasing protein concentrations are reached in the cuvette by consecutive addition of aliquots from a concentrate protein stock. In any case, the maximum protein concentration used in this ANS assay (4 μM) is substantially below the concentrations used in DLS, FTIR or gel filtration experiments ([HlyAΔ601] ≫ 25 μM). We have checked the more concentrated samples by QELS and we find that before and after a centrifugation step the particle diameters are virtually the same and correspond to the monomeric form of the protein (not shown). The values of maximum fluorescence emission (ΔF_{max}) were obtained from the $1/\Delta F$ vs. 1/[protein] double-reciprocal plot using increasing protein concentrations (0.2–4 μM) at a single (10 μM) ANS concentration [13].

The measured increase in fluorescence intensity, at 1 μM of protein and increasing ANS concentration, was translated into mol of bound ANS using the calibration factor. The data were then plotted using the Scatchard method ([ANS]bound/[ANS]free vs. [ANS]bound) and the dissociation constants (K_d) and the number of binding sites (n) were computed [14].

The calcium titration experiments were performed with 1 μM protein in TC buffer under the same conditions as those described above.

2.4. Trypsin digestion

Trypsin (swine, expressed in *Pichia pastoris*) was of proteomics grade (Roche, Manheim, Germany). Proteolysis of HlyAΔN601 was carried out at 30 °C in the presence or absence of 10 mM calcium chloride. The proteins were incubated with trypsin for 0, 15, 30 and 45 min and subsequently the reactions were stopped by the addition of 1 mM PMSF. The enzyme/protein mol ratio was 1/500. Degradation products were analyzed by SDS-PAGE (10 %) followed by staining with Coomassie Brilliant Blue.

2.5. Gel filtration by FPLC

Gel filtration was performed on a Superdex HR-200 column using a FPLC system (AKTA, GE Healthcare, USA). The protein (1 mg ml^{-1}) was dialyzed for 6 h in TC, TH or TCU buffer as required, where TCU buffer (Tris-calcium-urea) is a TC buffer which contains 6 M urea. The

samples were centrifuged at 18000*g* (20 min, 4 °C) in order to allow sedimentation of large protein aggregates. Then they were injected into the column which had previously been equilibrated with the appropriate buffer. The column was eluted at 0.5 ml min^{-1}.

2.6. Light scattering measurements

Quasi elastic light scattering (QELS) measurements were used to detect changes in protein size. The protein (1 mg ml^{-1}) was dialyzed overnight in TC, TH or TCU buffer as required. The samples were centrifuged at 18000*g* (20 min, 4 °C) in order to remove protein aggregates. QELS was measured at 25 °C, using a Zetasizer Nano-S (Malvern Instruments, Worcestershire, UK) at 633 nm.

Sample parameters as measured by QELS are the particle size or hydrodynamic diameter (D), and the polydispersity index (PDI). The particles in a colloidal sample are assumed to be spherical, monodisperse (i.e. of only a single size), and to diffuse following a Brownian motion. Both D and PDI values came out from the *cumulant analysis* (CA) of the intensity dispersed by the sample. The CA is the polynomial fit of the function $Ln[G1]=a+bt+ct^2+dt^3+et^4+(\ldots)$, where G1 is the correlation function of the scattering signal intensity. The coefficient of the squared term, *c*, when scaled as $2c/b^2$ is known as the *polydispersity*, or PDI. The diameter is the *Z*-average size of the CA, and corresponds to the particle size as calculated from the diffusion coefficient using the Stokes–Einstein equation [34]. PDI values range from 0 (monodisperse sample) to 1 (polydisperse, multimodal sample), and gives an estimation of the width of the size distribution, i.e. a narrow monomodal sample will have a value of e.g. 0.1, whereas in a broader distribution, most likely polymodal, the PDI will be over 0.5. Assuming a globular protein shape, the instrument calculates the molecular weight directly from the parameter D. For instance, an input of $D=3.76$ nm generates an output of 14.7 kDa, which is a good estimate for the size and molecular weight of lysozyme.

2.7. Infrared spectroscopy measurements

HlyAΔN601 was dialyzed against TC + 2 M urea buffer at 4 °C overnight. Then the protein solution was concentrated to 5 mg ml^{-1} using Millipore filters (30000 MW cut-off). In order to remove all the urea present in the sample, the concentrated protein was dialyzed against TC buffer at 4 °C for 6 h. The dialyzed proteins were centrifuged at 15,000*g* for 30 min at 4 °C to avoid protein aggregates. Protein aliquots (0.06 ml) were dried in a Savant evaporator (Labequip, Ontario, Canada). Finally they were resuspended in the appropriate volume of D_2O-based buffer and the infrared spectra were measured. The spectra were recorded in a Bruker Tensor 27 (Bruker Optik GmbH, Ettlingen, Deutschland) spectrometer equipped with a liquid nitrogen-refrigerated mercury-cadmium-telluride detector. Samples were measured using a demountable Peltier liquid cell (Biotools Inc., USA) with excavated calcium fluoride BioCell windows (BioTools), and 25 μm optical path. A total of 143 interferograms min^{-1} were generated at 2 cm^{-1} resolution and averaged over 1 min intervals. Opus 5.0 software from Bruker Optics was used for data acquisition. The sample was heated from 20 to 80 °C at a rate of 1 °C min^{-1}. Data treatment and band decomposition of the original amide I have been described elsewhere [15,16].

2.8. Urea denaturation measurements

The fluorescence emission of Trp was used to detect protein denaturation at increasing urea concentrations. Fluorescence was measured in a SLM Aminco 8100 spectrofluorometer. The excitation wavelength was 295 nm, and emission was scanned between 305 and 400 nm, with slits of 4 nm and 1 ml cuvettes with constant stirring were used. Protein stability was measured after the incubation of HlyA or the mutants (HlyAΔN601 and HlyAW914A) at increasing urea concentrations (0–8 M) in a TC buffer or TC + calcium (10 or 50 mM) for 2 h at 25 °C. The protein concentrations were 230 nM (HlyAΔN601) or 100 nM (HlyA and HlyAW914A).

In the case of the mutant HlyAΔN601 an additional experiment was carried out. The protein (230 nM) was dialyzed against TC or TC+1 mM calcium overnight at 4 °C, and then incubated at increasing urea concentrations (0–8 M) for 2 h at 25 °C.

Denaturation experiments were analyzed in terms of fractional denaturation,

$$f_D = \frac{\lambda_x - \lambda_N}{\lambda_D - \lambda_N}$$

where λ_x, λ_N, and λ_D are, respectively, the maximum fluorescence emission wavelengths of the protein Trp residues, of a partially denatured (λ_x), totally denatured (λ_D) or native protein (λ_N).

The denaturation constant K_D is:

$$K_D = \frac{f_D}{f_N} = \frac{f_D}{1-f_D}$$

Thus $\Delta G^0_D = -RT\ \ln K_D$, and the Gibbs free energy of protein denaturation, in the absence of urea, is $\Delta G^0_{H_2O} = \Delta G^\circ_D + m[\text{urea}]$, where m is an indicator of the extent to which the denatured state interacts with urea.

2.9. Intrinsic fluorescence measurements

The intrinsic fluorescence of HlyAΔN601 was used to detect conformational changes promoted by calcium binding at different urea concentrations. Fluorescence was measured in a SLM Aminco 8100 spectrofluorometer. The excitation wavelength was 295 nm, and emission was scanned between 305 and 400 nm, with slits of 4 nm and 1 ml cuvettes with constant stirring were used. Protein concentration was 100 nM, fluorescence was measured after equilibration (5 min) for each calcium concentration. The protein was dialyzed against TC + 6 M urea buffer in the presence of 0.1 mM EGTA at 4 °C overnight, and then against EGTA-free buffer for 2 h.

3. Results

3.1. Stabilizing effects of calcium in HlyAΔN601

3.1.1. ANS binding to HlyAΔN601

The effects of Ca^{2+} on the water-accessible hydrophobic regions of HlyAΔN601 were tested using 1,8-ANS (*1-anilino*-naphthalene-*8*-sulfonate). This is a water-soluble fluorescent probe, with a high affinity for hydrophobic regions in proteins, and on binding its fluorescence intensity (quantum yield) increases greatly, and the maximum wavelength of emission decreases correspondingly [13,17]. The protein was titrated with ANS both in the presence and absence of 10 mM Ca^{2+} and changes in probe fluorescence intensity were recorded (see Fig. S1A of the Supplementary Material). A preliminary inspection of the data indicates a larger increase in fluorescence intensity in the absence of Ca^{2+}. This suggests that the cation decreases the number of hydrophobic ANS-binding sites in the protein. Results from previous studies by this group using a Langmuir balance also suggested that, in the presence of Ca^{2+}, HlyAΔN601 became more hydrophilic [9].

Quantitative data on ANS binding to HlyAΔN601 were obtained using Scatchard plots [14]. For this purpose, values of maximum fluorescence emission (ΔF_{max}) were obtained using increasing protein concentrations (0.2–4 μM) at a single (10 μM) ANS concentration. ΔF_{max} was obtained from the $1/\Delta F$ vs. 1/[protein] double-reciprocal plot in Fig. 1A, and this was used to compute a calibration factor (ΔF_{max}/[ANS]). The latter value relates the change in fluorescence

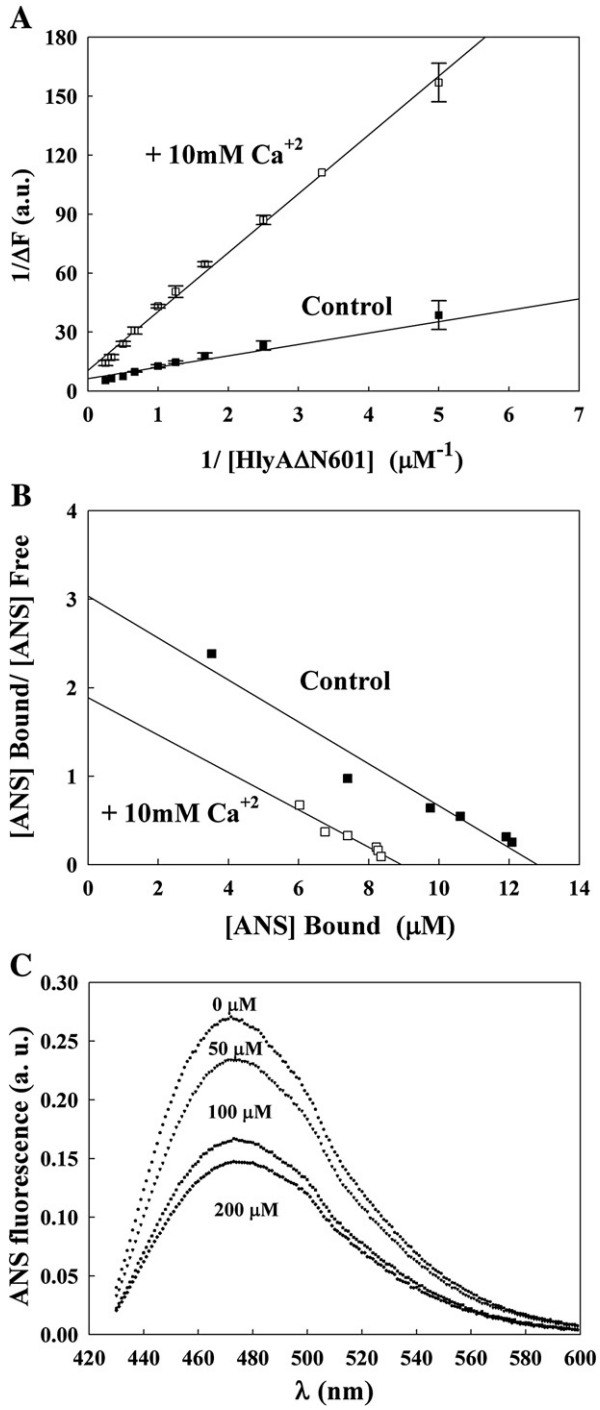

Fig. 1. ANS binding to HlyAΔN601. (A) Double-reciprocal plot of ANS fluorescence vs. HlyAΔN601 concentration. ANS concentration was 10 μM. Average values ± S.D. ($n = 2$). Regression coefficients: control, 0.98; buffer with 10 mM Ca^{2+}, 0.99. (B) Scatchard plot for values of bound ANS, obtained from data shown in Fig. SM1A. Regression coefficients: control, 0.95; buffer with 10 mM Ca^{2+}, 0.93. Average values of two closely similar representative experiments. (C) ANS fluorescence emission spectra in the presence of 1 μM protein, and increasing Ca^{+2} concentrations ($\lambda_{ex} = 360$ nm, $\lambda_{em} = 430$–600 nm).

intensity to the amount of protein-bound ANS. As shown in Fig. 1A, the experimental values obtained, in both the absence and presence of Ca^{2+} were 0.0157 and 0.0095 fluorescence units/μmol bound ANS respectively. This suggests a Ca^{2+}-induced change in the ANS-binding environment(s) of the protein.

Scatchard plots (Fig. 1B) allow the estimation of dissociation constants (K_d) and number of binding sites (n). In the absence of Ca^{2+}, it was found that $n = 12.7 \pm 1.0$ and $K_d = 4.2 \pm 1.1$ μM. The corresponding values in the presence of Ca^{2+} were $n = 9.0 \pm 0.1$; $K_d = 4.8 \pm 0.6$ μM. Thus our quantitative analysis confirms that Ca^{2+} decreases the number of ANS binding sites, i.e., the surface hydrophobicity of the C-terminal region of HlyA.

These observations were further explored and corroborated by titrating the protein-ANS complex, formed in the absence of Ca^{2+}, with increasing amounts of the cation (Fig. 1C). The probe fluorescence intensity decreased gradually with a minimum at ca. 200 μM Ca^{2+} (Supplementary Material, Fig. S1B). This was attributed to Ca^{2+} causing conformational changes in HlyAΔN601 that lead to a decrease in hydrophobic surfaces, and correspondingly in ANS binding sites, i.e., these results imply that Ca^{2+}-induced structural changes decrease ANS affinity for HlyAΔN601. It should be pointed out that the range of Ca^{2+} concentrations displacing ANS in these experiments is the same as that which has been found to cause an increase in the protein intrinsic fluorescence [9], and also the same as that which elicits the lytic activity of native HlyA [3].

ANS binding is a recognized method for estimating the number of "hydrophobic patches" in a protein surface [18]. For HlyAΔN601, the number of ANS binding sites decreases from 13 to 9 upon addition of Ca^{2+}, i.e., the protein surface is made less hydrophobic (Fig. 1). Note that even in the presence of Ca^{2+}, the number of ANS binding sites is high when compared with that of soluble proteins, such as pancreatic ribonuclease ($n = 1$), ovalbumin ($n = 1$) or lysozyme ($n = 3$). Bovine serum albumin, on the other hand, has $n = 10$, perhaps a reflection of its *in vivo* function as a carrier of fatty acids in the blood [13].

3.1.2. Calcium effects on the proteolytic digest of HlyAΔN601

HlyAΔN601 contains 44 putative cleavage sites for trypsin. In fact, the protein is readily hydrolyzed in the presence of trypsin at a 1/500 enzyme/protein mol ratio. However, as seen in Fig. 2, Ca^{2+} is very effective in protecting the protein against tryptic digestion. So, proteolytic digestion provides evidence for compaction of the Ca^{2+}-bound conformation. Ca^{2+} concentration in this and other experiments we carried out was 10 mM, which is much higher than the concentration required for optimum protein activity. This high Ca^{2+} concentration was chosen to compensate for various other effects, e.g., protein concentration, which varies according to the technique used, and the effect of urea which decreases HlyA affinity for Ca^{2+} (see below). Also, the use of 10 mM Ca^{2+} enables direct comparison of these results with those from our previous studies, in which the same calcium concentration was used.

3.1.3. Calcium effects on HlyAΔN601 apparent molecular mass and diameter

A study of the influence of calcium on the protein state of aggregation was carried out using molecular exclusion chromatography. The column was previously calibrated with protein standards of known molecular mass and Stokes radii. HlyAΔN601 was assayed in the presence and absence of 10 mM Ca^{2+}, and also in a buffer containing 6 M urea, in

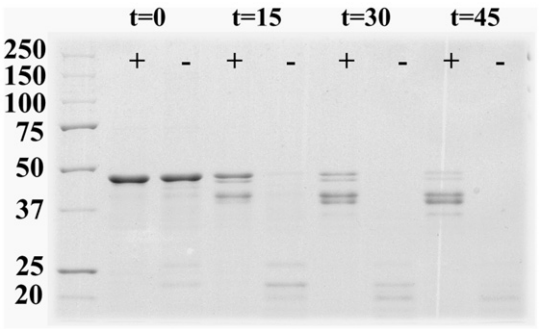

Fig. 2. Time course of HlyAΔN601 trypsin digestion. Electrophoretic patterns are shown for the protein, in the presence (+) and absence (−) of 10 mM Ca^{+2}, at 0, 15, 30 and 45 min after trypsin addition.

which the protein is usually stored [7,9]. Typical chromatograms of HlyAΔN601 protein under these different conditions are shown in Fig. 3. The protein elutes in very different ways according to the buffer composition. In the absence of Ca^{2+} (peaks marked "control") the protein is distributed across two peaks, one which elutes at 7.24 ml, very close to the column exclusion volume (7.2 ml), and another at 11.55 ml. However, in the presence of Ca^{2+}, a single peak eluting at 14.18 ml is observed I, while in the presence of urea the protein, in an unfolded state, elutes as a single peak at 9.42 ml.

From the elution volumes, and using the calibration curves obtained with the different buffers, the molecular mass and Stokes radii were determined for the protein. The molecular mass, as derived from its sequence, was found to be 46 kDa. The two peaks observed for HlyAΔN601 in the absence of Ca^{2+} had apparent molecular masses of 1698 kDa and 187.9 kDa and the latter had a Stokes radius of 48.6 Å. This latter peak is likely to correspond to a protein oligomer (maybe a tetramer), or perhaps a monomer with a very elongated shape, while the former represents some form of protein aggregate(s). In the presence of Ca^{2+} the apparent molecular mass was 47.1 kDa (Stokes radius 30.9 Å). So, in the presence of Ca^{2+} the protein elutes as a monomer, and its behavior is that of a globular protein. Finally, the apparent molecular mass of HlyAΔN601 in 6 M urea was 310.2 kDa, suggesting partial unfolding of the protein. These results are also compatible with the idea of Ca^{2+} making the protein more compact and reducing the hydrophobic areas in its surface, hence making it less prone to oligomerization.

The above results were investigated further and confirmed by examining the various protein preparations by quasi-elastic light scattering (QELS). The results are summarized in Table 1. In the presence of Ca^{2+}, the particles in suspension had an apparent molecular mass of 65 kDa, which may correspond to the protein in monomeric form, and this appears to be in good agreement with the results from the exclusion chromatography. In the absence of Ca^{2+}, the apparent molecular mass is much higher, about 80 times that of the monomer. This would correspond to the largest of the two fractions resolved by chromatography, i.e., the one that eluted close to the exclusion volume, and probably consisted of protein aggregates. The smaller fraction resolved in the chromatography column is not detected by QELS, presumably because light scattering by the larger particles masks the presence of other, smaller objects. In the presence of 6 M urea, the apparent diameter and molecular mass, i.e. 11.81 nm and 215 kDa, respectively, are higher than with calcium. Under these conditions, a higher value of PDI was determined (see Section 2.6), i.e. o.66, suggesting a heterogeneous collection of unfolded states.

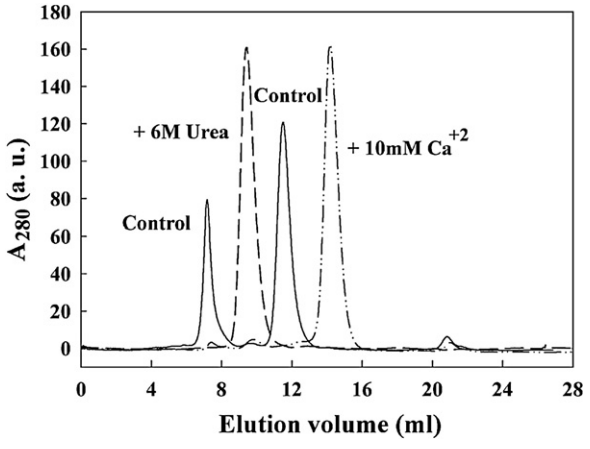

Fig. 3. Molecular exclusion chromatography of HlyAΔN601. Representative chromatograms, as the protein is eluted from a Superdex HR-200 column in buffers in the presence of 10 mM Ca^{+2} (– · · –), in the presence of 6 M urea (– –), or in the absence of either Ca^{+2} or urea (control, —).

Table 1
Dynamic light scattering of HlyAΔN601. The samples were dialyzed overnight in the appropriate buffer and centrifuged to remove macroscopic aggregates before the measurements were taken. The polydispersity index was calculated as described in Materials and methods (see Section 2.6).

Buffer	Diameter (nm)[a]	Polydispersity index[a]	Molecular weight (kDa)[b]
TC (No Ca^{+2}, no urea)	46 ± 5	0.24 ± 0.01	5000 ± 1000
TCU (No Ca^{+2}, 6 M urea)	11.81 ± 0.08	0.66 ± 0.04	215 ± 3
TH (10 mM Ca^{+2}, no urea)	7.1 ± 0.1	0.44 ± 0.05	65 ± 3

[a] Average values ± S.D. of three independent measurements.
[b] Estimated from the apparent diameters, assuming globular protein shape.

3.1.4. Calcium effects on HlyAΔN601 thermal stability, as detected by IR spectroscopy

In our previous study [9] we used IR spectroscopy to describe the structural effects of Ca^{2+} on the truncated protein, namely the increase in the fraction of secondary structure corresponding to β-sheet and α-helix, at the expense of non-periodic and loop structures. In this study we carried out a similar analysis as a function of temperature, over the 20–80 °C range. Representative spectra at low and high temperatures, in the presence and absence of Ca^{2+}, are given in the Supplementary Material, Fig. S2, whilst the percentage distribution of secondary structure components is shown in Table 2. In general, thermal changes are less pronounced in the presence of Ca^{+2} (Supplementary Material Fig. S2A and C) than in its absence (Supplementary Material Fig. S2B and D). It is worth noting here that heating HlyAΔN601 up to 75 °C did not give rise to prominent aggregation (intermolecular contacts) bands at ca. 1620 and 1685 cm^{-1} [15,19].

In the absence of the cation, the main effect of temperature was an increase in the proportion of α-helix (from 10% to 22%) and a concomitant decrease, of about the same magnitude, in disordered structure (from 18% to 3%; Table 2). Protein thermal denaturation is often accompanied by an increase in the proportion of the periodic α and β structures [15]. However, in the presence of Ca^{+2} the observed changes are too small to be meaningful in this context.

Thermal denaturation of proteins as detected by IR spectroscopy is often observed by plotting the amide I band width-at-half-height as a function of temperature. In previously studied proteins, denaturation was marked by an abrupt increase in width, due to the appearance of intense aggregation bands at 1620 and 1685 cm^{-1} [15]. As discussed above, these bands do not seem to be as prominent in HlyAΔN601 as

Table 2
Secondary structure (amide I band components) of HlyAΔN601 at 25 °C and 75 °C in the presence and absence of Ca^{2+}, as derived from IR spectroscopy. Virtually superimposable spectra were obtained from different protein preparations. The data in the table correspond to a representative series of spectra obtained with the same protein batch. Values have been rounded off to the nearest integer. Data at 25 °C taken from Sanchez-Magraner et al. [9].

Assignment	−Ca^{2+}				+Ca^{2+}			
	25 °C		75 °C		25 °C		75 °C	
	Position		Position		Position		Position	
	cm^{-1}	% Area	cm^{-1}	% Area	cm^{-1}	% Area	cm^{-1}	% Area
High-frequency intermolecular contacts + β-turns	1684	6	1685	7	–	–	–	–
High-frequency β-sheet β-turns	1673	7	1675	5	1679	6	1682	4
β-turns	1663	12	1665	13	1669	6	1670	10
α-helix	1654	10	1651	22	1659	18	1660	15
Disordered	1644	18	1641	3	1648	8	1649	12
β-sheet (low-frequency component)	1629	32	1631	32	1633	57	1633	53
Intermolecular contacts (+ Tyr)	1614	15	1614	18	1613	5	1613	6

they are in most proteins. The width vs. temperature plot for the protein in the presence and absence of Ca^{2+} is shown in Fig. 4. In the absence of Ca^{2+}, a broad denaturation event is seen to take place between ca. 42 and 62 °C. The presence of 10 mM Ca^{2+} reduces the amide I band width considerably at all temperatures, and suppresses denaturation over the temperature range used in our study. Thus Ca^{2+} clearly makes the structure of HlyAΔN601 more compact and thermally stable.

3.2. Urea unfolding of HlyA and HlyAΔN601

We have shown in a previous study that urea gradually unfolded native HlyA, with 6–8 M urea leading to a fairly stable form that could be stored for months at −20 °C [7]. Conveniently, unfolding can be monitored as an increase in the intrinsic fluorescence emission wavelength λ_{max} of the protein. The same procedure can be applied to the study of urea unfolding of HlyAΔN601. As shown in Fig. 5A, the emission spectrum in the absence of Ca^{2+} ("control") was shifted, by about 16 nm, to higher wavelengths by 8 M urea. In the presence of Ca^{2+}, as shown previously [9] the intensity of the fluorescence emission increases by ca. 3-fold. With 8 M urea there was a shift towards a higher λ_{max} of emission, but also a large decrease in intensity (Fig. 5A). This decrease in intensity, which occurs only in the presence of Ca^{2+}, can be seen when looking in more detail as in Fig. 5B. As a result, the emission spectra of HlyAΔN601 in 8 M urea in the presence or absence of Ca^{2+} shown in Fig. 5A are virtually superimposed.

The latter result could be interpreted in terms of urea decreasing the protein affinity for Ca^{2+}. This explanation is supported by the results shown in Fig. 6. It can be seen that Ca^{2+} caused the expected increase in fluorescence intensity, with a half-maximal effect at about 50 μM at 0.06 M urea, i.e., a urea concentration resulting from diluting in the spectroscopic cuvette the HlyAΔN601 stock, usually kept in 6 M urea. However, when urea concentrations in the cuvette were increased to 0.5 M or 1 M, Ca^{2+} concentrations required to induce a similarly enhanced fluorescence intensity also increased. So, as seen in Fig. 6, more Ca^{2+} is required in the presence of urea to reach the compact state induced by Ca^{2+}. The observation of this urea/Ca^{2+} effect can also explain previous data for native HlyA [7], according to which the native protein was more stable against urea denaturation in a "haemolysis buffer" containing 10 mM Ca^{2+}, than in the "control buffer," in the absence of the cation.

Intrinsic fluorescence emission data of HlyA and related proteins in the presence of increasing urea concentrations can be readily normalized and converted into data of fractional denaturation (f_D) (Fig. 7A and B). The stabilizing effect of Ca^{2+} is illustrated by the large increase in urea concentration required to cause 50% denaturation ($f_D = 0.5$): 2.84 M and 5.86 M for HlyAΔN601 in the absence or presence

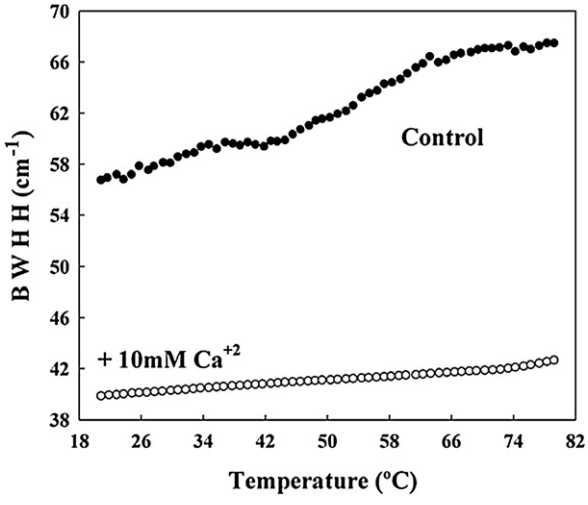

Fig. 4. Thermal denaturation of HlyAΔN601 in the presence and absence of 10 mM Ca^{+2}. Data derived from IR spectra (amide I bands) as seen in supplementary Fig. S2. Amide I band width at half-height is plotted versus temperature. Average values of two closely similar representative experiments.

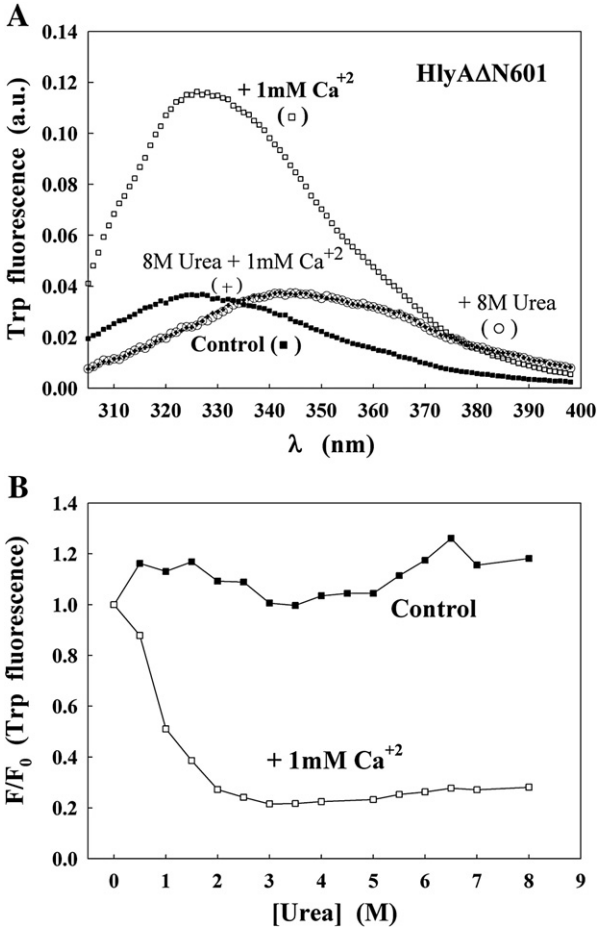

Fig. 5. Urea denaturation of HlyAΔN601. Ca^{2+} displacement by urea. (A) Intrinsic fluorescence emission spectra in the presence of 1 mM Ca^{+2} (□), in the presence of 8 M urea (○), in the presence of 1 mM Ca^{+2} + 8 M urea (+) and, control in the absence of both calcium and urea (■). Note that the spectra in the presence of 8 M urea (○) and in the presence of 1 mM Ca^{+2} + 8 M urea (+) are virtually superimposed. (B) The change in relative intrinsic fluorescence emission intensities in the presence (□) and absence (■) of Ca^{2+}, as a function of urea concentration. Average values of two closely similar representative experiments.

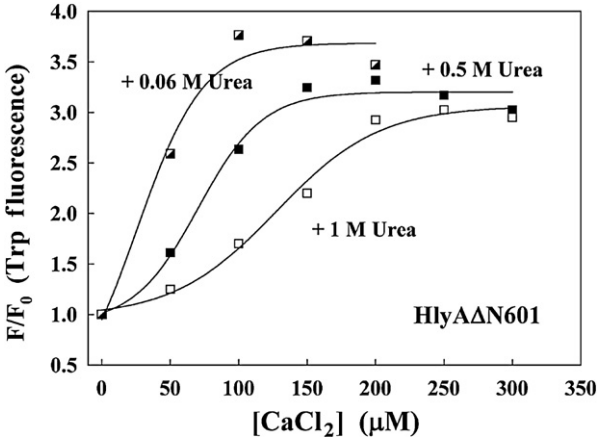

Fig. 6. The effect urea on Ca^{2+} binding. Ca^{2+}-dependent enhancement of intrinsic fluorescence intensity of HlyAΔN601 at increasing urea concentrations. Data are shown from one of two closely similar experiments, performed with different protein preparations.

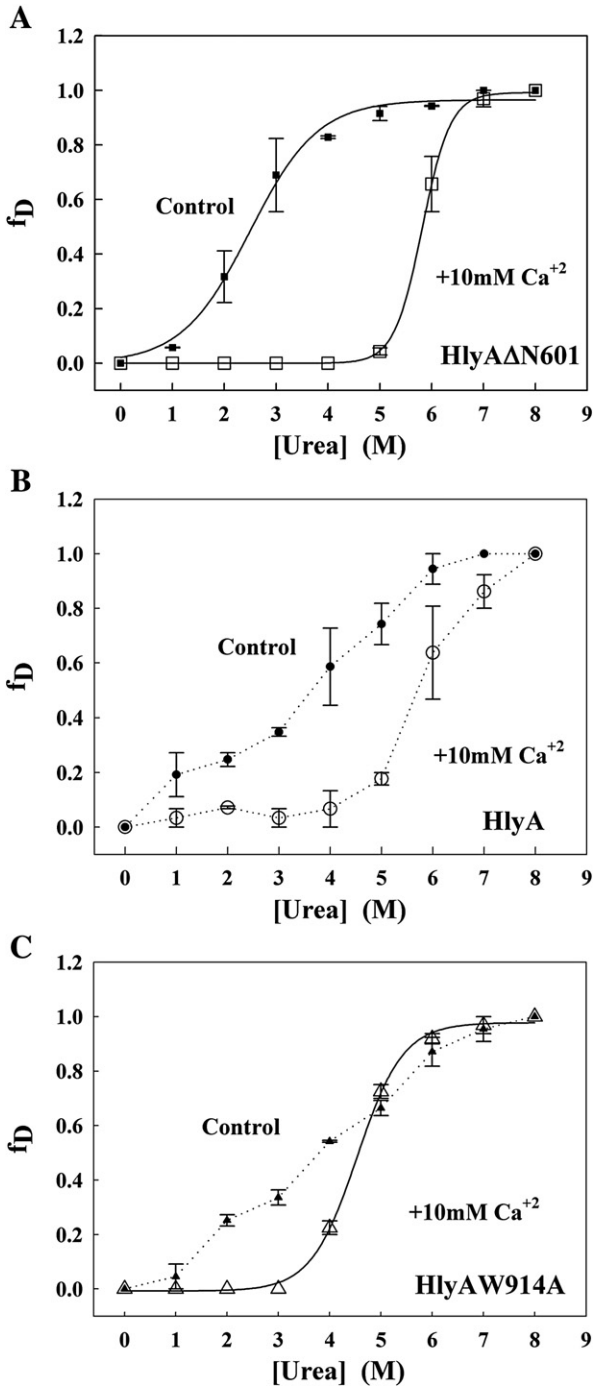

Fig. 7. Urea denaturation of native HlyA and of the two main domains in the presence and absence of Ca^{2+}. (A) HlyAΔN601 (B) HlyA. (C) HlyA W914A. Fractional denaturation f_D (see Materials and methods for details) is plotted vs. urea concentration in the presence (open symbols) or absence (closed symbols) of Ca^{2+}. Average values ± S.D. ($n = 2$).

of 10 mM Ca^{2+} respectively, and 3.2 M and 5.6 M for native HlyA under equivalent conditions. From f_D data, in the favorable case when denaturation approaches a two-state model, the Gibbs free energy of unfolding ($\Delta G^0_{H_2O}$) can be computed. This is the case for HlyAΔN601 in the presence of Ca^{2+}, in which case $\Delta G^0_{H_2O} = 12.1 \pm 1.2$ kcal/mol.

For the correct interpretation of the plots in Fig. 7A and B it should be noted that the Trp residues indicating urea unfolding are not the same in each case. The C-terminal moiety of HlyA, HlyAΔN601, contains a single Trp residue (position 914 in the native protein), while native HlyA contains, in addition, three other Trp residues at positions 432, 480 and 579. Thus the unfolding data from Fig. 7A correspond specifically to the C-terminal nonapeptide repeat domain, while those in Fig. 7B report also on the unfolding of the N-terminal region containing the amphipathic helices [7,8].

3.3. Urea unfolding of HlyA W914A

In order to obtain specific information on the unfolding of the N-terminal region within the whole protein, a mutant was prepared in which Trp914 was replaced by Ala. So, denaturation of HlyA W914A followed through changes in intrinsic fluorescence should essentially indicate changes occurring in the amphipathic helices region.

The lytic activities of the mutant, both on liposomes and on red blood cells, were comparable to those of native HlyA (Supplementary Material, Figs. S3A and B) although HlyA W914A required slightly more Ca^{2+} (approximately 200 μM) for full activity (Supplementary Material, Fig. S4). The mutant bound liposomes and became inserted in phosphatidylcholine monolayers spread at the air–water interface just as the native protein (data not shown). Interestingly, the intrinsic fluorescence of HlyA W914A did not change in the presence of Ca^{2+}, up to concentrations of 500 μM (Supplementary Material, Fig. S5) although, as mentioned above, 200 μM Ca^{2+} was enough to induce full lytic activity. The fact that the mutant does not exhibit the characteristic Ca^{2+}-dependent increase in intrinsic fluorescence of HlyA [3] reveals that the latter effect occurs largely, if not exclusively, at the level of the NRD.

Urea unfolding of HlyA W914A is illustrated in Fig. 7C. In the absence of calcium the denaturation curve for this mutant is complex and non-cooperative, rather similar to the curve observed for the native protein under the same conditions. In the presence of calcium, however, the Trp residues in the N-terminal amphipathic domain, where no high-affinity calcium-binding sites exist, indicate a stabilizing effect of Ca^{2+} on this mutant. Furthermore, in the presence of the cation the denaturation curve of HlyA W914A can be fitted to a two-state model curve, indicative of cooperativity in the denaturation process ($\Delta G^0_{H_2O} = 5.0 \pm 0.1$ kcal/mol). The stabilizing effect exerted on the N-terminal part of the protein by calcium binding to the NRD indicates a long-range effect of Ca^{2+}, which extends from the C-terminal to the N-terminal domain of HlyA.

4. Discussion

The two main observations in this paper are (i) that Ca^{2+} stabilizes the C-terminal region of HlyA, containing the nonapeptide repeat domain (NRD) that is characteristic of the RTX protein family, and (ii) that Ca^{2+} binding to the repeat domain helps fold and stabilize the N-terminal domain of the protein. Calcium binding has three major effects on HlyAΔN601, the C-terminal moiety of HlyA consisting mainly of the NRD: it makes the protein surface on average more hydrophilic (Fig. 1, Table 1); it causes the molecule to fold in a more compact form, as a globular monomer (Fig. 2, Table 2); and it increases its thermal stability (Fig. 4). It should be noted that, even in the presence of Ca^{2+}, the number of "hydrophobic patches" on the protein surface, estimated from ANS binding, is higher than in soluble proteins, in agreement with the high surface activity of HlyAΔN601 [9].

In relation to the more compact folding induced by Ca^{2+}, the IR spectra (Fig. S3, Table 2) provide data that explains previous X-ray crystallographic observations with related RTX proteins. The IR results indicate that Ca^{2+} promotes major changes in the secondary structure of the protein, with an increase in the periodically ordered patterns α and β, and a decrease in the more flexible unordered structures and loops. This is interpreted as the protein in the presence of Ca^{2+} folding to form a β-sheet cylinder, in which the Ca^{2+} ions are located between adjacent loops, thus stabilizing the fold (β-roll) [4]. There are abundant examples of proteins, apart from members of the RTX

family, whose structure is known to be stabilized through cation binding [20,21]. Conversely, the cation-depleted apoprotein is often far less stable, as shown for concanavalin and Ca^{2+} [20]. Chenal et al. [22] have recently described a similar effect on the NRD of adenylate cyclase toxin from *Bordetella pertussis*, another member of the RTX family.

The formation of stable secondary and tertiary structures of proteins is dictated by intramolecular interactions between the constituent amino acid residues and their interaction with the surrounding medium [23]. From the classical studies by Tanaka and Scheraga [24] inter-residues interactions are classified into short-, medium- and long-range, according to the separation between the residues along the polypeptide chain. The importance of long-range interactions for determining the folding rate of proteins has been underlined by Gromika and Selvaraj [25]. The folding of multi-domain proteins, such as HlyA, presents a further degree of complexity, since inter-domain interactions must also be taken into account [26]. The available data suggest that the slowest step in the folding of large proteins is the intramolecular assembly of the (partially) folded domains [27]. This may be due to the domains being incompletely folded before the final assembly occurs, to the fact that H_2O molecules need to be removed between domains which must also be in close contact in the final structure, or to other energetically unfavorable events [28]. The importance of partial dehydration of domain surfaces in the final folding has been quantitatively assessed by Zhou et al. [29]. HlyA is a two-domain protein, and the data in Figs. 5–7 in this paper clearly indicate that Ca^{2+}-induced folding of the NRD helps in turn fold the N-terminal domain, making this part of the protein more stable. No high-affinity Ca^{2+}-binding sites have been found in the N-terminal domain of α-haemolysin, so the Ca^{2+} effect in the C-terminal domain is being transmitted to the amino end of the protein. It is interesting to note that in the low-density lipoprotein receptor, the N-terminal ligand-binding region, composed of seven complement-like domains each stabilized partly by one calcium atom, acquires its native conformation late in folding, and its post-translational folding leads to the last step of the lipoprotein receptor sequential folding [30]. There are other indications of multidomain proteins in which Ca^{2+}-binding to one or more domains favors the complete protein folding, e.g. a basement membrane glycoprotein [31], the glycoprotein fibrillin-1 [32], and members of the βγ-crystallin superfamily [33]. For HlyA though, direct evidence has been presented in this paper that links Ca^{2+} binding to one domain and the thermodynamic stabilization of a second domain, as well as of the whole protein. It is conceivable that Ca^{2+} plays a similar role in other members of the RTX protein family, all of them containing a high-affinity Ca-binding domain and at least one additional functional domain. The calcium-induced conformational switch between partially unfolded conformations in the absence of calcium, and stable structures in the presence of this cation is likely to be a key property for the biological function of HlyA and the other toxins of the RTX family. It can be conceived that under in vivo bacterial conditions, with a low intracellular calcium concentration and a very crowded bacterial cytosol, the synthesis and export of such large, hydrophobic polypeptides must be tightly coupled in such a way that the unfolded calcium-free, aggregation-prone conformation is not likely to exist as such, unless protected by some kind of intracellular chaperones. However once the protein leaves the bacterium towards the calcium-rich extracellular milieu, binding of calcium to the C-terminal repeats domain, that might function as a folding nucleator, would ensure achieving the folded, active conformation of the protein toxin.

Acknowledgments

This work was supported in part by the Spanish Ministerio de Educación y Ciencia (grant No. BFU 2007-62062 and grant No. BFU 2006-14423) and by the University of the Basque Country (grant No.GIU 06/42). DMG was supported by the Bizkaia Xede program. LSM was an I3P predoctoral student from the Consejo Superior de Investigaciones Científicas.

Appendix A. Supplementary data

Supplementary data associated with this article can be found, in the online version, at doi:10.1016/j.bbamem.2010.03.007.

References

[1] C. Balsalobre, J.M. Silvan, S. Berglund, Y. Mizunoe, B.E. Uhlin, S.N. Wai, Release of the type I secreted alpha-haemolysin via outer membrane vesicles from *Escherichia coli*, Mol. Microbiol. 59 (2006) 99–112.
[2] R.A. Welch, RTX toxin structure and function: a story of numerous anomalies and few analogies in toxin biology, Curr. Top. Microbiol. Immunol. 257 (2001) 85–111.
[3] H. Ostolaza, A. Soloaga, F.M. Goni, The binding of divalent cations to *Escherichia coli* alpha-haemolysin, Eur. J. Biochem. 228 (1995) 39–44.
[4] U. Baumann, S. Wu, K.M. Flaherty, D.B. McKay, Three-dimensional structure of the alkaline protease of *Pseudomonas aeruginosa*: a two-domain protein with a calcium binding parallel beta roll motif, EMBO J. 12 (1993) 3357–3364.
[5] T. Hege, U. Baumann, Protease C of *Erwinia chrysanthemi*: the crystal structure and role of amino acids Y228 and E189, J. Mol. Biol. 314 (2001) 187–193.
[6] R. Meier, T. Drepper, V. Svensson, K.E. Jaeger, U. Baumann, A calcium-gated lid and a large beta-roll sandwich are revealed by the crystal structure of extracellular lipase from *Serratia marcescens*, J. Biol. Chem. 282 (2007) 31477–31483.
[7] A. Soloaga, J.M. Ramirez, F.M. Goni, Reversible denaturation, self-aggregation, and membrane activity of *Escherichia coli* alpha-hemolysin, a protein stable in 6 M urea, Biochemistry 37 (1998) 6387–6393.
[8] A. Soloaga, M.P. Veiga, L.M. Garcia-Segura, H. Ostolaza, R. Brasseur, F.M. Goni, Insertion of *Escherichia coli* alpha-haemolysin in lipid bilayers as a non-transmembrane integral protein: prediction and experiment, Mol. Microbiol. 31 (1999) 1013–1024.
[9] L. Sanchez-Magraner, A.R. Viguera, M. Garcia-Pacios, M.P Garcillan, J.L. Arrondo, F. de la Cruz, F. M Goni, H. Ostolaza, The calcium-binding C-terminal domain of *Escherichia coli* alpha-hemolysin is a major determinant in the surface-active properties of the protein, J. Biol. Chem. 282 (2007) 11827–11835.
[10] L. Bakas, M.P. Veiga, A. Soloaga, H. Ostolaza, F.M. Goni, Calcium-dependent conformation of *E. coli* alpha-haemolysin. Implications for the mechanism of membrane insertion and lysis, Biochim. Biophys. Acta 1368 (1998) 225–234.
[11] C. Schindel, A. Zitzer, B. Schulte, A. Gerhards, P. Stanley, C. Hughes, V. Koronakis, S. Bhakdi, M. Palmer, Interaction of *Escherichia coli* hemolysin with biological membranes. A study using cysteine scanning mutagenesis, Eur. J. Biochem. 268 (2001) 800–808.
[12] C. Bauche, A. Chenal, O. Knapp, C. Bodenreider, R. Benz, A. Chaffotte, D. Ladant, Structural and functional characterization of an essential RTX subdomain of *Bordetella pertussis* adenylate cyclase toxin, J. Biol. Chem. 281 (2006) 16914–16926.
[13] M. Cardamone, N.K. Puri, Spectrofluorimetric assessment of the surface hydrophobicity of proteins, Biochem. J. 282 (1992) 589–593.
[14] G.B. Reddy, K.P. Das, J.M. Petrash, W.K. Surewicz, Temperature-dependent chaperone activity and structural properties of human alphaA- and alphaB-crystallins, J. Biol. Chem. 275 (2000) 4565–4570.
[15] J.L. Arrondo, A. Muga, J. Castresana, F.M. Goni, Quantitative studies of the structure of proteins in solution by Fourier-transform infrared spectroscopy, Prog. Biophys. Mol. Biol. 59 (1993) 23–56.
[16] J.L. Arrondo, F.M. Goñi, Structure and dynamics of membrane proteins as studied by infrared spectroscopy, Prog. Biophys. Mol. Biol. 72 (1999) 367–405.
[17] M.S. Celej, G.G. Montich, G.D. Fidelio, Protein stability induced by ligand binding correlates with changes in protein flexibility, Protein Sci. 12 (2003) 1496–1506.
[18] D. Matulis, C.G. Baumann, V.A. Bloomfield, R.E. Lovrien, 1-anilino-8-naphthalene sulfonate as a protein conformational tightening agent, Biopolymers 49 (1999) 451–458.
[19] J.L. Arrondo, N.M. Young, H.H. Mantsch, The solution structure of concanavalin A probed by FT-IR spectroscopy, Biochim. Biophys. Acta 952 (1988) 261–268.
[20] D.I. Stuart, K.R. Acharya, N.P. Walker, S.G. Smith, M. Lewis, D.C. Phillips, Alpha-lactalbumin possesses a novel calcium binding loop, Nature 324 (1986) 84–87.
[21] M. Kikuchi, K. Kawano, K. Nitta, Calcium-binding and structural stability of echidna and canine milk lysozymes, Protein Sci. 7 (1998) 2150–2155.
[22] A. Chenal, J.I. Guijarro, B. Raynal, M. Delepierre, D. Ladant, RTX calcium binding motifs are intrinsically disordered in the absence of calcium: implication for protein secretion, J. Biol. Chem. 284 (2009) 1781–1789.
[23] T.R. Obalinsky, Protein folding: New research, Nova Science Publishers Inc., New York, 2006.
[24] S. Tanaka, H.A. Scheraga, Model of protein folding: inclusion of short-, medium- and long-range interactions, Proc. Natl. Acad. Sci. USA 722 (1975) 3802–3806.
[25] M.M. Gromika, S. Selvaraj, Importance of long-range interactions for determining the folding rate and transition state structures of two-state proteins, Genome Inform. 13 (2002) 348–349.
[26] J.H. Han, S. Batey, A.A. Nickson, S.A. Teichmann, J. Clarke, The folding and evolution of multidomain proteins, Nat. Rev. Mol. Cell Biol. 8 (2007) 319–330.
[27] J. Garel, Folding of large proteins: multidomain and multisubunit proteins, in: T. Creighton (Ed.), Protein Folding, Freeman, New York, 1992, pp. 405–454.
[28] T.E. Creighton, Proteins: structures and molecular properties, Freeman, New York, 1983.

[29] R. Zhou, X. Huang, C.J. Margulis, B.J. Berne, Hydrophobic collapse in multidomain protein folding, Science 305 (2004) 1605–1609.
[30] A. Jansen, E. van Duijn, I. Braakman, Coordinated nonvectorial folding in a newly synthesized multidomain protein, Science 298 (2002) 2401–2403.
[31] P. Maurer, U. Mayer, M. Bruch, P. Jeno, K. Mann, R. Landwehr, J. Engel, R. Timpl, High-affinity and low-affinity calcium binding and stability of the multidomain extracellular 40-kDa basement membrane glycoprotein (BM-40/SPARC/osteonectin), Eur. J. Biochem. 205 (1992) 233–240.
[32] P. Whiteman, A.C. Willis, A. Warner, J. Brown, C. Redfield, P.A. Handford, Cellular and molecular studies of Marfan syndrome mutations identity co-operative protein folding in the cbEGF12-13 region of fibrillin-1, Hum. Mol. Genet. 16 (2007) 907–918.
[33] K. Itoh, M. Sasai, Cooperativity, connectivity, and folding pathways of multidomain proteins, Proc. Natl. Acad. Sci. USA 105 (2008) 13865–13870.
[34] K. Schmitz, An Introduction to Dynamic Light Scattering by Macromolecules, Academic Press, San Diego, 1990.